# Measured Impedance Characteristics of Solar Inverters up to 1 MW

Soenke Rogalla
Fraunhofer Institute for Solar Energy Systems ISE
Heidenhofstraße 2, 79110 Freiburg
Email: soenke.rogalla@ise.fraunhofer.de

Sebastian Kaiser
Fraunhofer Institute for Solar Energy Systems ISE
Heidenhofstraße 2, 79110 Freiburg
Email: sebastian.kaiser@ise.fraunhofer.de

Bruno Burger
Fraunhofer Institute for Solar Energy Systems ISE
Heidenhofstraße 2, 79110 Freiburg
Email: bruno.burger@ise.fraunhofer.de

Bernd Engel
TU Braunschweig
Universitätsplatz 2, 38106 Braunschweig
Email: Bernd.Engel@tu-braunschweig.de

***Abstract*—This paper presents an enhanced measurement technique and its application for determining the harmonic characteristics of inverters. With the suggested test method of *differential impedance spectroscopy* the inverter can be described as a frequency-dependent Thévenin equivalent. Thus, the output impedance and internal harmonic sources can be determined frequency wise. Having this, one can analyze the harmonic interactions between inverters and the grid more precisely. It allows to distinguish between so-called resonance-based harmonics, which result from the effective inverter and grid impedance constellation, and source-driven harmonics, which are introduced by harmonic sources on the inverter or the grid side. First this paper explains the principle of differential impedance spectroscopy and the calculation of the inverter's Thévenin equivalents. Finally it presents and discusses the measured results from different commercial PV inverters in a power range up to 2.5 MVA.**

***Index Terms*—Impedance spectroscopy, impedance based stability, stability analysis, harmonic sources, output impedance of inverters, grid stability**

## I. Introduction

With the increasing expansion of renewable energies, the share of power electronics based generators is growing. Already today more than 100 GW of wind and PV power plants are connected to the German electricity grid [1]. Together with the integration of electrolysis plants, battery storage and HVDC transmission systems, a connected inverter capacity of over 500 GW is expected until 2030 based on the plans of the German government [2]. A major technical challenge for the future energy system is to ensure stable network operation and maintain high voltage quality. However, problems with critical harmonic content in PV and wind parks can already be observed, which are due to electrical resonance formation between inverters and the grid. The European transmission grid operators ranked the top ten power system stability issues. Three of the ten problems deal with resonances between cables and passives components, interactions between controllers and power oscillations [3]. With established methods for determining harmonic emissions, however, almost no statements can be made about possible resonances and the associated consequences. There are different approaches to determine harmonic emissions by using the impedance characteristic of the solar inverters [4], [5]. The required impedance curves can determined by measurement, analytically or by simulation [6]. This paper concentrates on measuring the output impedance of inverters by means of a new measuring technique called differential impedance spectroscopy. This method allows to determine frequency-dependent Thévenin equivalents of an inverter, i.e. the determination of its output impedance as well as the internal harmonic sources. Thereby the interfering influences of given harmonic sources

The presented work was financially supported by the German Federal Ministry for Economic Affairs and Energy under the project number 0325757F („Netzharmonie“)

on the impedance measurements can be compensated leading to more reliable measurement results. Impedance curves measured in this way can be used to analyze resonance situations, e.g. by means of the impedance-based stability criterion. In addition the measured Thévenin voltages can be used for an improved assessment of the harmonic emissions of inverters.

In section II the procedure of the *impedance spectroscopy of inverters* will be explained in general. Examples of measured Thévenin equivalents of different inverters are presented below, with section III comparing the determined impedance curves and section IV discussing the identified internal harmonic sources of the analyzed inverters.

## II. Impedance Spectroscopy of Inverters

Impedance spectroscopy is a proven method for the characterization of dielectric materials, e.g. in fuel cells or batteries [7]. It is based on the assumption that the system under investigation can be described by a network of passive components. For this purpose, an small-signal AC voltage is applied to the system and the resulting current response is measured. The frequency $f_{exc.}$ of the excitation voltage is step-wise increased. With the given excitation voltage and the measured current response the $V/I - ratio$ of the system for each frequency step can be calculated. Having a passive system the $V/I - ratio$ equals the impedance of the system. However, when analyzing active systems like inverters further factors must be considered. First of all, the device under test (DUT) must be set into operation by providing a fundamental voltage (50 Hz or 60 Hz). The excitation voltage must then be superimposed on this fundamental voltage. Figure 1 shows the single line representation of a possible test setup for impedance spectroscopy of inverters. The currents and voltages are measured at the terminals of the DUT and transformed into the frequency domain. Only the voltages and the current components of the actual excited frequency are taken into account for the further analysis. When calculating the $V/I - ratio$ of inverters, one will find significant discontinuities and distortions in the resulting curve. This can be explained by the presence of harmonic sources inside the inverter.

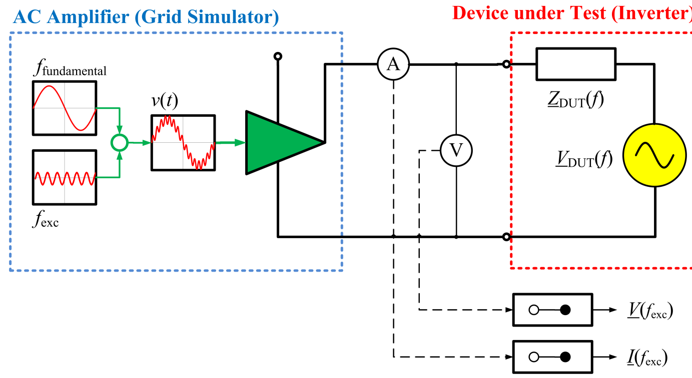

Figure 1: Principle test setup for impedance spectroscopy of inverters (single line representation) [8].

To solve this problem, the inverter is described as a Thévenin equivalent for each frequency. Hence, the task is to determine both the serial output impedance $Z_{DUT}(f)$ and inner voltage source $V_{DUT}(f)$ of the inverter. To determine the two unknown variables two independent measurements are necessary. Independent measurements can be obtained by varying amplitude and/or phase angle of the excitation voltage for each frequency. Having the measured voltage $\underline{V}_A(f)$ and current $\underline{I}_A(f)$ for the first excitation as well as for the second excitation ($\underline{V}_B(f)$ and $\underline{I}_B(f)$), the searched values for $Z_{DUT}(f)$ and $V_{DUT}(f)$ can be calculated according to equation (1) and (2), respectively.

$$\underline{Z}_{DUT}(f) = \frac{\underline{V}_B(f) - \underline{V}_A(f)}{\underline{I}_B(f) - \underline{I}_A(f)} \tag{1}$$

$$\underline{V}_{DUT}(f) = \frac{\underline{V}_A(f) \cdot \underline{I}_B(f) - \underline{V}_B(f) \cdot \underline{I}_A(f)}{\underline{I}_B(f) - \underline{I}_A(f)} \tag{2}$$

Since $Z_{DUT}$ represents the differential impedance of the DUT in the given operation point, this approach is called *differential impedance spectroscopy* [8]. The advantage of this method is demonstrated impressively in Figure 2. The figure shows the difference between the $V/I - ratio$, which was obtained from the regular impedance spectroscopy of an exemplary solar inverter, and the determined Thévenin impedance for the same inverter using the differential impedance spectroscopy. While the $V/I - ratio$ shows discontinuities at different frequencies, these peaks are completely removed in characteristic of $Z_{DUT}(f)$.

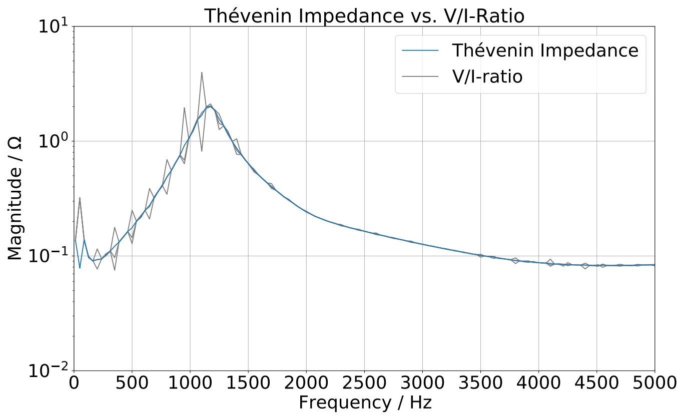


Figure 2: Comparison of the $V/I - ratio$ obtained by a regular impedance spectroscopy and the Thévenin Impedance $Z_{DUT}(f)$ of an exemplary solar inverter with a nominal power of 1 MVA.

## A. Evaluation in symmetrical components

When analyzing three-phase inverters, it is possible and recommended to determine the Thévenin equations in symmetrical components. However, in order to receive the negative sequence impedance it is necessary to excite the DUT with a negative sequence voltage. If the DUT has a neutral wire connection a zero sequence excitation and analysis is possible, too. It has been shown that it is not required to excite all frequencies with positive, negative and zero sequence voltages, but to concentrate on the natural harmonic sequences. Natural harmonic sequences create the same voltage shape in the three phases. Their relation between the symmetrical components and the harmonic order are given in Table I. The analysis of the Thévenin equivalents presented in the following section haven been performed in symmetrical components.

Table I: Natural sequence harmonics

| Sym. component | Harmonic order | Frequencies [Hz] for $f_{fund}$ =50 Hz |
|---|---|---|
| Positive sequence | $3k+1$ | 50, 200, 350, 500,... |
| Negative sequence | $3k-1$ | 100, 250, 400, 550,... |
| Zero sequence | $3k$ | 150, 300, 450, 600,... |
| | for k=1,2,3,... | |

## III. Comparison of different impedance curves of solar inverters

This chapter presents the results of the determined Thévenin equivalents of different inverters. All devices are three-phase solar inverters in the power range of 10 kVA to 2.5 MVA. Beside the power rating the DUTs differ in their bridge and filter topologies as well as in their switching frequency. Table II gives a list of the seven analyzed inverters with their properties. The table lists up the nominal power $S_N$, the operating power during the impedance spectroscopy $P_{OP}$, the filter topologies and the switching frequencies $f_{switch}$. The results of the impedance determination by means of the above-mentioned differential impedance spectroscopy are presented in Figure 3 for the analyzed inverters. The figure shows beside the positive also the negative sequence components (dashed lines) of the Thévenin impedances. Except the very low frequency range and a special serial resonance point of DUT 7 the positive and negative impedance do not differ significantly for the investigated inverters. As a first general conclusion, the size of the impedance correlates with the nominal power as expected, i.e. high-power inverters tend to show lower output impedance. Furthermore all devices have at least one parallel resonance point, whereas its position and form differ between the devices. Peaks in the impedance curve typically originate from parallel resonance of the LC filter. This behaviour can also be observed in the phase angle, where the phase shows a transition from inductive (90°) to capacitive range (–90°) at the respective resonance frequency. It is important to note, that the shape of the impedance can be affected by the inverter's controller maximum up to the half of the switching frequency according to Shannon's theorem. Hence, resonance points within this frequency range is typically actively attenuated by the controller. However, above this frequency range, the impedance is defined solely by the behavior of the passive filter components. It can be mentioned, that DUT 5 and DUT 7 show an additional resonance point at higher frequencies. This is caused by a second filter choke of the LCL filter or the differential choke of the EMC filter.

Finally one can say, that it is not possible to predict, if an inverter runs stable based on its impedance

Table II: Devices under test and their parameters

| DUT No. | $S_N$ | $P_{OP}$ | Filter topology | $f_{switch}$ |
|---|---|---|---|---|
| DUT 1 | 36 kVA | 33 kW | LC | 16 kHz |
| DUT 2 | 23 kVA | 23 kW | LC | 16 kHz |
| DUT 3 | 10 kVA | 10 kW | LC | 16 kHz |
| DUT 4 | 1 MVA | 500 kW | LCR | 4 kHz |
| DUT 5 | 60 kVA | 60 kW | LCL | 15 kHz |
| DUT 6 | 150 kVA | 150 kW | LC | 8 kHz |
| DUT 7 | 2.5 MVA | 500 kW | LC | 3 kHz |

characteristic alone and without having information about the surrounding impedance situation. Nevertheless, in order to reduce tendency for resonances with the grid or other neighboring inverters, a reasonable resistive part of the impedance is beneficial, i.e. frequencies at which an inverter behaves almost pure inductive or capacitive have a high risk to form weakly damped resonances.

Among the analyzed inverters DUT 1, DUT 2 and DUT 5 are the only ones with an neutral line connection. Hence, zero sequence analysis is possible for those inverters. Figure 4 shows the results of the zero sequence determination. Comparing the positive, negative and zero sequence for DUT 2 one can find, that all three impedances are almost the equal. This is due to the fact, that this inverter is able to control all three phases independently. Thus, the inverter reacts on any symmetrical component excitation in a same manner. In contrast, DUT 1 and DUT 5 show significant higher impedance values for the zero sequence than for the positive and negative sequence impedances. Obviously this inverter is not able to control the zero sequence current freely. The neutral connection is probably only used to connect the output filters. In this case the zero sequence impedance is defined mainly by the filter values. In general, care must be taken when

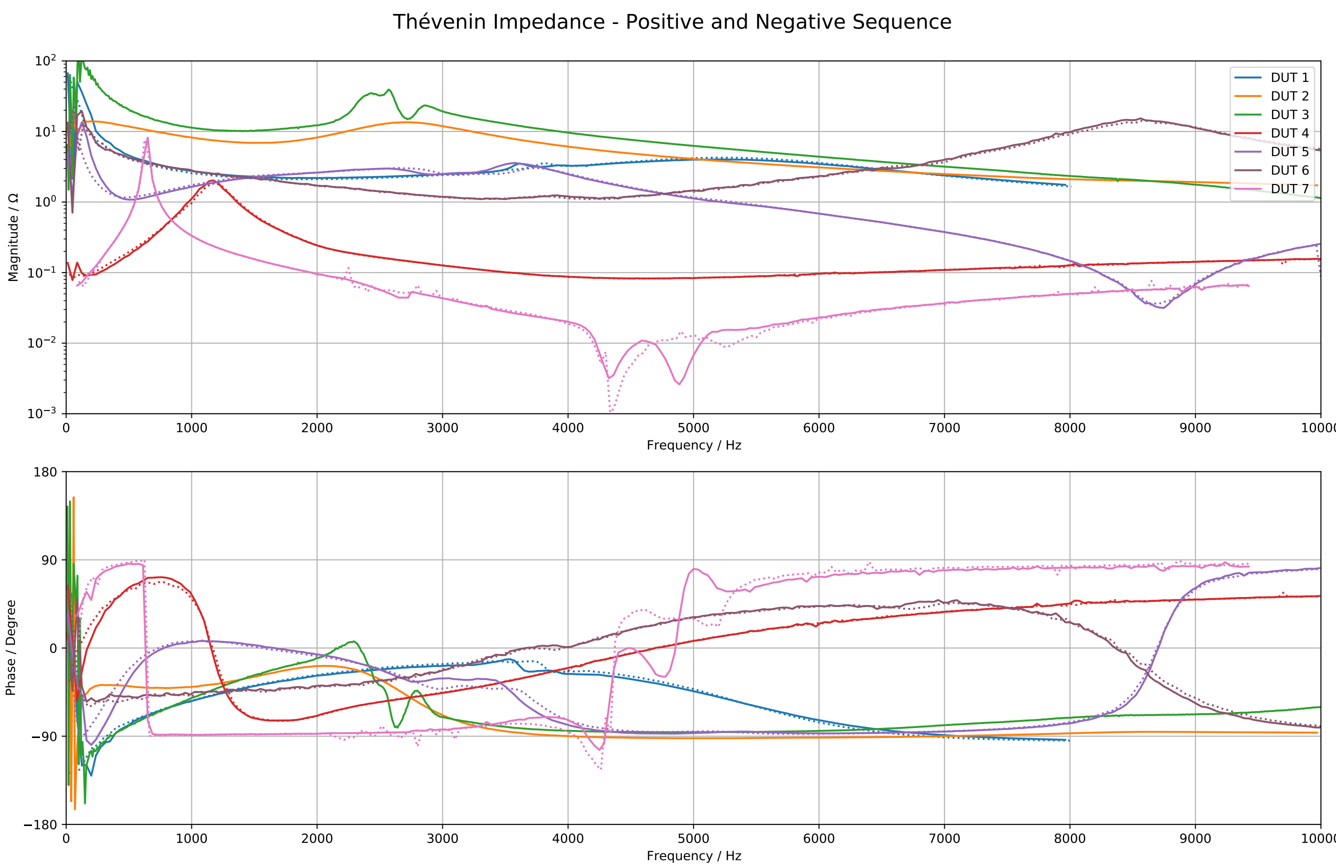


Figure 3: Measured Thévenin impedances of seven different solar inverters in a power range between 10 kVA and 2.5 MVA. Bold lines show the positive sequence impedances, whereas dashed lines represent the negative sequences impedances.

interpreting zero-sequence impedances, as devices connected on the DC supply side of the inverter may influence the results.

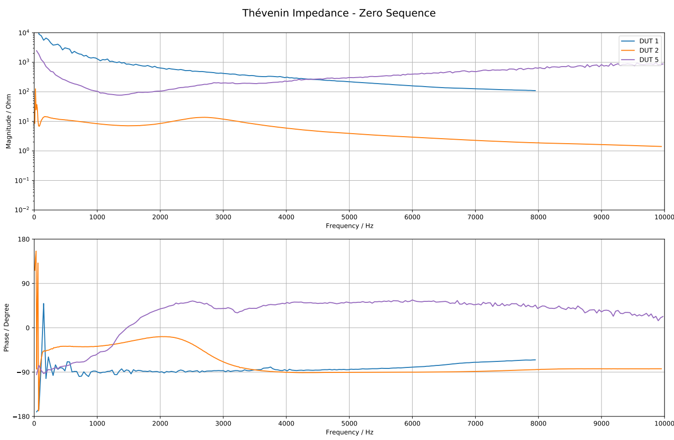


Figure 4: Measured zero sequence impedances of DUT 1, DUT 2 and DUT 5.

## IV. Comparison of the Thévenin Voltages

Although today's inverters are of very high power quality, power electronic devices contain certain internal harmonic sources. This can be caused by various effects, which include non-linearities of the main choke [9] or the inverter bridge, e.g blanking time [10] and zero current clamping effects [11]. Furthermore there are switching frequency related sources [12] and sources introduced by the control, e.g. controllers for the reduction of selected harmonics. Figure 5 shows exemplary the measured spectrum of the Thévenin voltage of DUT 1.
The inverter shows considerable voltage amplitudes only for the uneven harmonic orders. The voltage levels drop rapidly and have largely decayed by 1 kHz. Although the Thévenin voltages depend on the above-mentioned internal harmonic sources, they are not the same, because they are additionally influenced by the output impedance. This circumstance can be illustrated by the results of DUT 4 shown in Figure 6. The amplitudes of the Thévenin voltages reach its peak at 1.1 kHz, which is exactly the frequency at which the impedance curve of this inverter shows its maximum (cf. Figure 3). Considering that the LC output filter of the inverter contains a capacitor as a parallel element, which has to be converted into a representing serial element according to Thévenin's theorem, it explains why

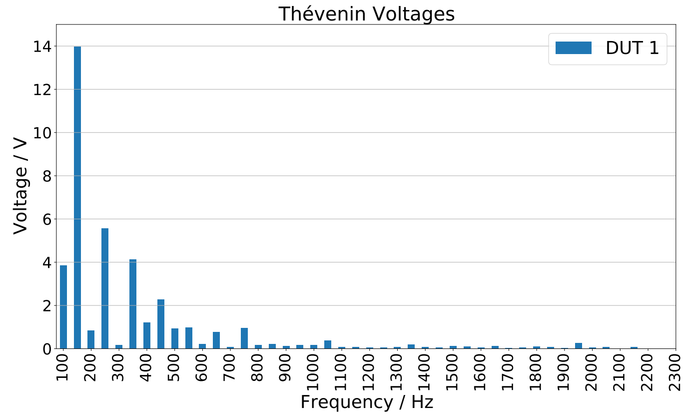


Figure 5: Measured Thévenin voltages of DUT 1. The shown values are alternating the positive, negative and zero sequence voltages according to Table I.

relatively small physical harmonic sources of the inverter bridge can show increased Thévenin voltage levels at frequencies around the filter resonance point. This shows that it is not suitable to use only the Thévenin voltage spectra as a basis for an evaluation of the harmonic emission of inverters. In order to develop an improved assessment method both the Thévenin voltages and impedances must be considered, e.g. by evaluating the calculated harmonic short-circuit currents.

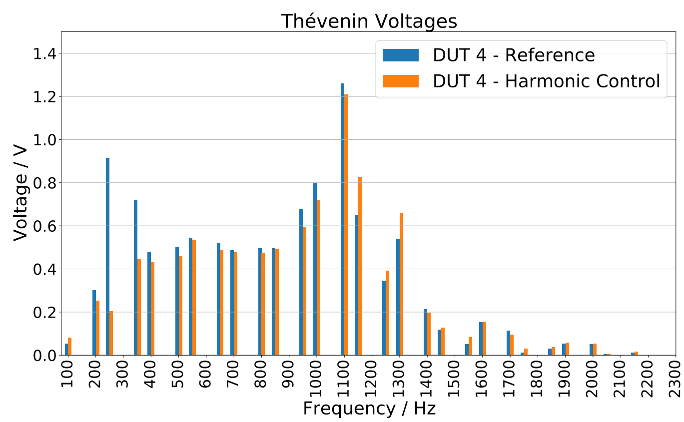


Figure 6: Spectra of the Thévenin voltages of DUT 4 with and without activated harmonic controller.

Figure 6 depicts another interesting finding. It shows the results of the Thévenin Voltages for two different controller configurations of DUT 4. The device provides a special harmonic controller, which allows to reduce the fifth and seventh harmonic of its output current. The reference spectrum was obtained while this harmonic controller was disabled, whereas during a second spectroscopy it was activated. Hence, the reference spectrum (blue) shows significantly larger levels for the fifth and seventh order (250 Hz and 350 Hz) than the second spectrum (orange), where the harmonic controller was enabled. As expected, the effect of the harmonic controller can be observed in the Thévenin voltage spectrum.

## V. Conclusion

The presented differential impedance spectroscopy is a new method to analyze the harmonic characteristic of an inverter by determining its frequency-dependent Thévenin equivalents. It has been shown, that the output impedance curves measured with the new approach show much better results as the regular impedance measurement techniques. This makes it possible to use the determined impedance curves to analyze resonance-based harmonics. In contrast to existing methods, the influence of the grid impedance on the harmonic current spectrum can be analyzed now. The harmonic spectrum of the Thévenin voltages delivered by the differential impedance, spectroscopy is a promising basis to develop improved methods for the evaluation of harmonic emissions for inverters.

This paper presented measurement results of seven different inverters and it has shown that the output impedance can differ significantly. Influencing factors like the switching frequency, the nominal power and the filter design as well as the control were discussed. When analyzing the Thévenin impedances and voltages of three-phase inverters it is suitable to use symmetrical components, since positive, negative and zero sequence characteristic may differ.

In summary this paper showed that the metrological determination of the frequency-dependent Thévenin equivalents of inverters is possible even in a megawatt-scale and that the achieved results can help to better analyze harmonic interactions between inverters and the grid.

## References


[1] Bruno Burger, "Energy charts," 2020. [Online]. Available: https://energy-charts.info/index.html?l=de&c=DE

[2] Bundesregierung Deutschland, "Klimaschutzprogramm 2030 der bundesregierung zur umsetzung des klimaschutzplans 2050," 2019. [Online]. Available: https://www.bundesregierung.de/breg-de/themen/klimaschutz/klimaschutzprogramm-2030-1673578

[3] S. Rüberg, V. Sewdien, J. Rueda Torres, D. Wang, B. Tuinema, N. Farrokhseresht, R. Meyer, A. Mertens, L. Hofmann, D. Herwig, and T. Breithaupt, "Migrate deliverable d1.1: Report on systemic issues." [Online]. Available: https://www.h2020-migrate.eu/

[4] J. Sun, "Impedance-based stability criterion for grid-connected inverters," *IEEE Transactions on Power Electronics*, vol. 26, no. 11, pp. 3075–3078, 2011.

[5] S. Rogalla, F. Ackermann, N. Bihler, H. Moghadam, and O. Stalter, "Source-driven and resonance-driven harmonic interaction between pv inverters and the grid," *43rd Photovoltaic Specialists Conference (PVSC)*, 2016.

[6] X. Wang, L. Harnefors, and F. Blaabjerg, "Unified impedance model of grid-connected voltage-source converters," *IEEE Transactions on Power Electronics*, vol. 33, no. 2, pp. 1775–1787, 2018.

[7] S. Ma and S. Boggs, "50+ years of impedance measurement and spectroscopy, and implementation of virtual spectroscopy based on finite element analysis," *IEEE Electrical Insulation Magazine*, vol. 30, no. 1, pp. 25–31, 2014.

[8] S. Rogalla, S. Kaiser, B. Burger, and B. Engel, "Determination of the frequency dependent thévenin equivalent of inverters using differential impedance spectroscopy," *IEEE International Symposium on Power Electronics for Distributed Generation Systems; PEDG*, vol. 11th, 2020.

[9] M. Bienholz and G. Griepentrog, "Prediction of harmonic current frequencies and amplitudes generated in power inductors due to saturation in ferrite and iron powder cores," in *2016 IEEE 2nd Annual Southern Power Electronics Conference (SPEC)*. IEEE, 05.12.2016 - 08.12.2016, pp. 1–4.

[10] Y. Murai, A. Riyanto, H. Nakamura, and K. Matsui, "Pwm strategy for high frequency carrier inverters eliminating current clamps during switching dead-time," in *Conference Record of the 1992 IEEE Industry Applications Society Annual Meeting*, IEEE Power Electronics Society, Ed. IEEE, 4-9 Oct. 1992, pp. 317–322.

[11] K. Wiedmann, "Positionsgeberloser betrieb von permanentmagneterregten synchronmaschinen," Dissertation, Gottfried Wilhelm Leibniz Universität Hannover, Hannover, 2012.

[12] D. Schulz, *Netzrückwirkungen - Theorie, Simulation, Messung und Bewertung: Nach DIN VDE 0838, DIN VDE 0839 und den VDEW-Richtlinien mit Simulationsbeispielen in Simplorer und Messbeispielen von netzgekoppelten Photovoltaik- und Windkraftanlagen*, 2nd ed., ser. VDE-Schriftenreihe Normen verständlich. Berlin: VDE-Verl., 2004, vol. 115.